ROCK MASS CHARACTERIZATION FOR EXCAVATIONS IN MINING AND CIVIL ENGINEERING

By Nick Barton, Ph.D.[1]

ABSTRACT

When the Q-system was launched in 1974, the name referred to rock mass classification, with focus on tunnel and cavern support selection. Besides empirical design of support, the Q-value, or its normalized value Q_c, has been found to correlate with seismic P-wave velocity, with deformation modulus, and with deformation. The Q-system provides temporary or permanent support for road, rail, and mine roadway tunnels and for caverns for various uses. It also gives relative cost and time for tunnel construction for a complete range of rock qualities. There are also indications that Q has captured important elements of the cohesive and frictional strength of rock masses, with Q_c resembling the product of rock mass cohesion and rock mass friction coefficient.

ROCK MASS VARIABILITY

From the outset, the Q-system has focused on sound, simple empiricism that works because it reflects practice and that can be used because it is easily remembered. It is appropriate to start by illustrating the widely contrasting rock mass qualities that may challenge both the civil and mining professions, fortunately not on a daily basis, but therefore also unexpectedly.

Figure 1 shows a core box from a project that has not been completed during 10 years of trying. The massive core is from a project that may not be started for at least 10 years. The first should already have passing high-speed trains; the other may have high-level nuclear waste some time in the future. They are both from the same country, but may have six orders of magnitude contrast in Q-value. A second pair of examples shown in Figure 2 requires a cable car for access on the one hand, and successive boat trips to fault-blocked flooded sections of tunnel on the other.

The contrasting stiffness and strength of intact rock and wet clay is easy to visualize. One may be crushed by one and drowned in the other. There are sad and multiple examples of both in the tunneling and mining industries. They merit a widely different quality description, as for instance given by the wide range of the Q-value.

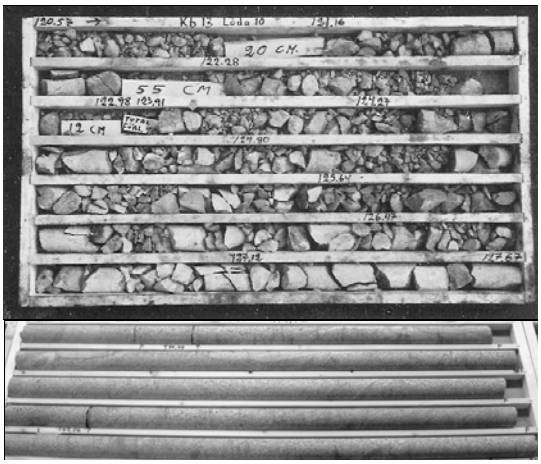

Figure 1.—The contrast shown by these two core boxes suggests orders of magnitude differences in quality. Quantitative descriptions of shear strength and deformation modulus would vary by orders of magnitude as well. Quality descriptors like RMR or GSI that suggest qualities differing from only 5 to 95, or 10 to 90, cannot then be as appropriate as the 0.001–1000 range of Q seen in these examples. Increasing the range of Q to Q_c adds further reality, since Q_c might range from 0.0005 to 2500 in these two cases.

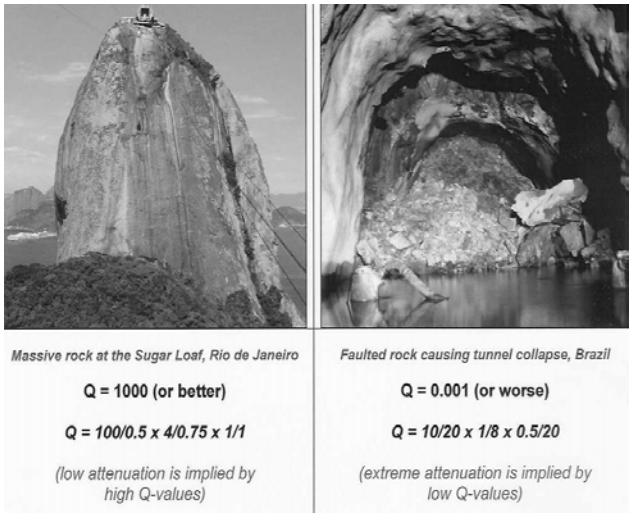

Figure 2.—Respective access by cable car and by boat, emphasizes the need for radically different magnitudes of rock quality and also radically different magnitudes of seismic quality, the inverse of attenuation [Barton 2006]. A single project beneath Hong Kong harbor demonstrated a length of core of 57 m without a joint and an even wider regional fault zone. With such extremes, RQD values of 100% and 0% are clearly inadequate, too, but can clearly be improved by using local Q-values of, for example, 1000 and 0.001.

[1]President, Nick Barton & Associates, Høvik, Norway.

The term Q is composed of fundamentally important parameters (Figure 3) that were each (besides Deere's Rock Quality Designation (RQD)) quantified by exhaustive case record analysis. The six orders of magnitude range of Q is a partial reflection of the potentially enormous variability of geology and structural geology. It is probably because of the relative sensitivity of a classification that can show wide numerical variation (i.e., 10^{-3} to 10^{3}, or an even wider range using $Q_c = Q \times \sigma_c/100$) that correlation with a very varied geologic and hydrogeologic reality is achieved, using rather simple correlations. Without this range of Q (approximately 10^{6}) or Q_c (approximately 10^{9}), correlation would be more complex, as it seems to be with the Geological Strength Index (GSI) in particular, since this is based on the limited numerical range of the Rock Mass Rating (RMR) system.

$$Q = \frac{RQD}{J_n} \times \frac{J_r}{J_a} \times \frac{J_w}{SRF}$$

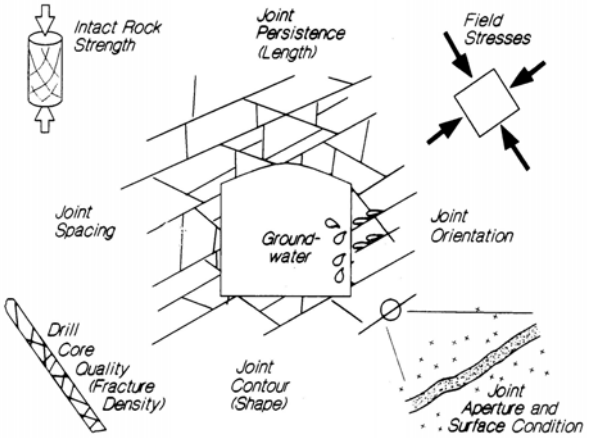

Figure 3.—A pictorial representation of the Q-parameters, from Hutchinson and Diederichs [1996]. The modern application of the Q-system [Barton 2002] includes both indirect and direct use of UCS. When the rock strength-to-stress ratio is unfavorable, in the case of massive (high RQD/J_n) rock masses, the SRF value will need to be very high to represent excavation difficulties, i.e., deep-shaft excavation, due to potential stress slabbing or minor bursting. The high SRF and correspondingly low Q-value require heavy yielding support. In the case of jointed rock under high stress, SRF will not need to be so high.

COMMON ASPECTS OF OVERBREAK AND CAVABILITY IN MINING

Figure 4 shows the fundamental importance of the number of sets of joints and their roughness using the Q-system parameters J_n (number of sets) and J_r (roughness). This figure also shows overbreak (and therefore large-scale cavability, in principle) caused by three sets of joints, but with the important proviso that without a degree of joint

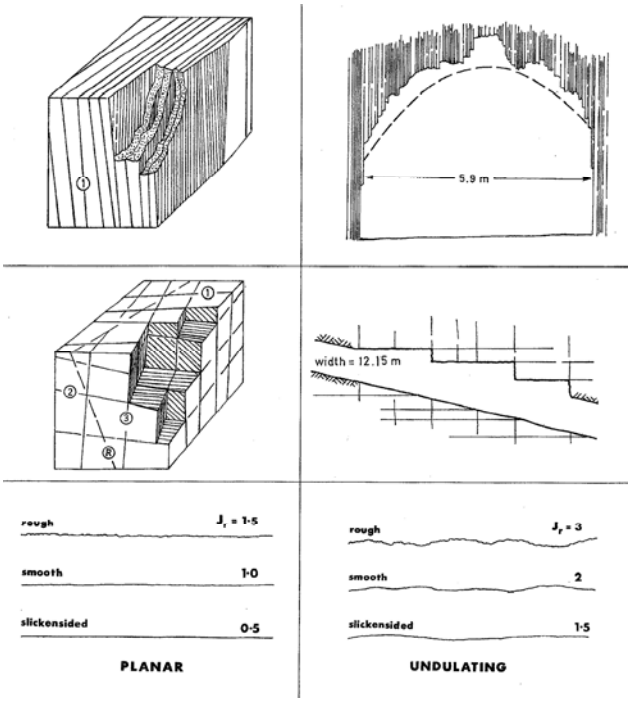

Figure 4.—Two of the most important components of Q and of rock mass stability are the number of joint sets (or degree of freedom for block definition and fallout) and the joint roughness (or interblock release-or-hold mechanism). The general level of overbreak and ease of carrying out characterization in tunnels are also fundamentally affected by these two parameters. In the case of block caving in mining, the ratio J_n/J_r is fundamental for initiating such mechanisms.

surface planarity, neither overbreak in a tunnel/roadway, nor block caving are likely to occur without significant assistance.

It is quite likely that, whatever the overall Q-value at a given (potential) block caving locality in an ore body, the actual combination J_n/J_r will need to be ≥6 for successful caving (e.g., 6/1, 9/1.5, 12/2), while such combinations as 9/3 might prove to be too dilatant. Even four joint sets (J_n = 15) with too high J_r (such as 3) would probably prejudice caving due to the strong dilation and need for a lot of long-hole drilling and blasting. Significantly, this last ratio (15/3 = 5) is also <6.

The simple J_r description shown in Figure 4, when combined with J_a, also gives a realistic estimate of the interblock friction angle, as illustrated in Figure 5. These parameters form part of the first and second pairs of parameters describing the Q-value. (RQD/J_n = relative block size, J_r/J_a = interblock friction coefficient). Obviously, a combination of J_n = 6 to 9 (or more), and J_r = 2, 1.5, or less, *and* J_a ≥1 would be ideal attributes for block caving and equally *unfavorable* for overbreak and tunnel or cavern support needs, where permanent, or temporary, stability was required.

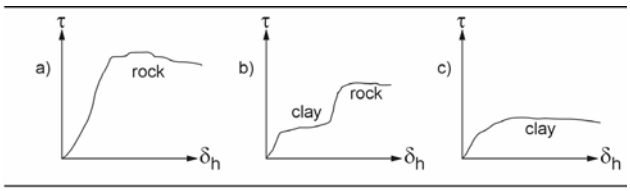

(a) Rock wall contact (thin coatings)

J_a/J_r =	0.75	1.0	2	3	4
	$\tan^{-1}(Jr/Ja)°$				
A. Discontinuous joints	4	79°	76°	63°	53°	45°
B. Rough, undulating	3	76°	72°	56°	45°	37°
C. Smooth, undulating	2	69°	63°	45°	34°	27°
D. Slickensided, undulating	1.5	63°	56°	37°	27°	21°
E. Rough, planar	1.5	63°	56°	37°	27°	21°
F. Smooth, planar	1.0	53°	45°	27°	18°	14°
G. Slickensided, planar	0.5	34°	27°	14°	9.5°	7.1°

(b) Rock wall contact when sheared (thin fillings)

J_a/J_r =	4	6	8	12
	$\tan^{-1}(Jr/Ja)°$			
A. Discontinuous joints	4	45°	34°	27°	18°
B. Rough, undulating	3	37°	27°	21°	14°
C. Smooth, undulating	2	27°	18°	14°	9.5°
D. Slickensided, undulating	1.5	21°	14°	11°	7.1°
E. Rough, planar	1.5	21°	14°	11°	7.1°
F. Smooth, planar	1.0	14°	9.5°	7.1°	4.7°
G. Slickensided, planar	0.5	7°	4.7°	3.6°	2.4°

Figure 5.—A graphic demonstration of the workings of J_r and J_a in the context of joint or clay-filled discontinuity friction angles. For minimal overbreak and tunnel support needs, J_r/J_a needs to be as large as possible. For block caving, a mostly "category a" (rock-to-rock joint wall contact) friction angle is expected. The J_r values (the vertical columns of ratings on the left side) will need to be 2 or less; otherwise, dilation during shear will stop block caving from occurring, unless block size is small enough for block rotation to occur, e.g., Barton [2004].

CONSEQUENCES OF OVERBREAK IN A CAVERN AND IN A MINE

The 62-m span Gjøvik Olympic cavern in Norway typically had J_n/J_r of 9/2, and it was stable with the help of bolting and shotcrete and a favorable (horizontal) stress situation. Although it suffered significant overbreak, J_n/J_r of 9/2 prevented caving, i.e., locally excessive overbreak. With J_n/J_r of 9 (three sets) and J_r of 1 (planar), the project would have had another degree of complexity, i.e., it would have caved at the very wide face, without close-to-the-face rock support. Of course, the magnitude of RQD (where RQD/J_n represents relative block size) and the details of J_a (possible clay-filling or soft mineralization) will modify the above simplicity; hence the use of Q.

The typical Gjøvik cavern J_n/J_r ratio (9/2 = 4.5), although not allowing caving (or uncontrolled overbreak) during blasting, did allow overbreak of 1 to 2 m, as seen through the 10 cm of S(fr) in the 62-m span arch seen about 20 m above the camera location in Figure 6. In such overbreak locations, there was invariably a local J_n = 12–15 (up to four sets) character, with J_r of about 2, i.e., a ratio of J_n/J_r of ≥ 6. This implies the likely need for support in civil engineering excavations and mine roadways, while in the case of block caving, could signal relative ease of caving initiation, as shown in the following example.

Figure 6.—Example of a well-jointed rock mass with most typically J_n = 9 (three sets of joints) and J_r = 2, seen in the Gjøvik Olympic cavern of 62-m span. Note the deep overbreak in the 25-m-high arch and the use of B + S(fr) permanent support [Barton et al. 1994].

In the steeply inclined Kiruna ore body in Sweden, the Q-system parameters were evaluated by systematic logging in >2 km of upper-level long-hole drilling galleries and in corresponding ore-loading galleries at the base of the proposed LKAB Oscar (long-hole block caving) project [Barton 1988]. Roughness characterization of the jointing exposed by failed zones (extreme overbreak) in the drifts due to inadequate temporary support was used to evaluate the possibility of larger-scale block release and caving disruption, as illustrated schematically at the top of Figure 7 (see "J1" and "J2" areas).

As may be noted from the Q-histogram logging illustrated in Figure 7, the most frequent J_n/J_r ratings were 9/2. This proved insufficient for unassisted caving. Drift failures (few) tended to have occurred with J_n/J_r of, for example, 12/1.5, sometimes with the additional facilitation of J_a = 3, i.e., mineralized joints.

The above ratings for the various joint and rock mass parameters for the two example projects illustrate behavior with respect to overbreak and cavability—the former at stress levels of 3–5 MPa (Gjøvik Olympic cavern), the latter at 15–20 MPa (Kiruna's LKAB Oscar project). Clearly, high initial and developing stress levels expected in a deep mine may give a necessary "boost" to block fracturing and interblock friction mechanisms, thereby demonstrating the need for block stress-fracturing and joint stress-propagation mechanisms, if initiation of caving should be modeled.

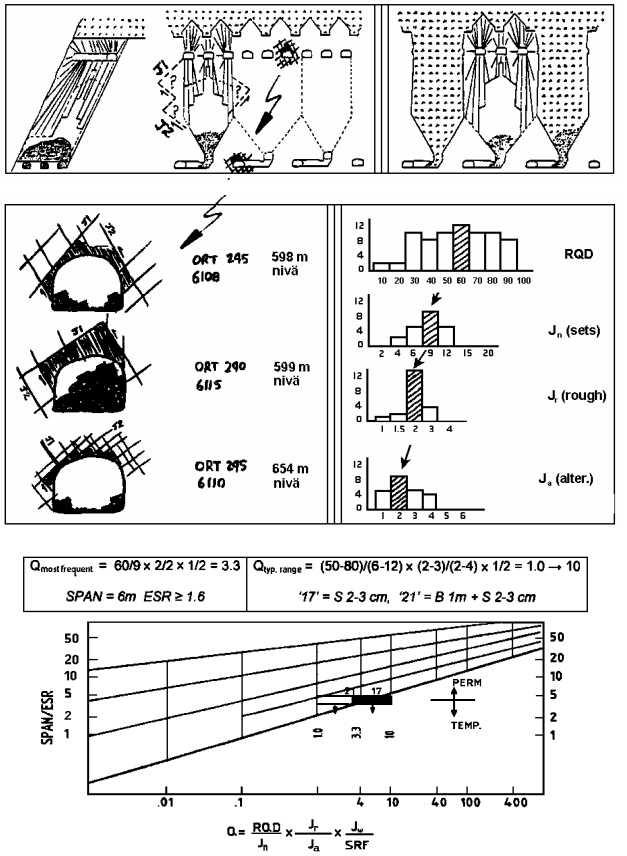

Figure 7.—Kiruna's LKAB Oscar long-hole caving project. Some details of rock mass Q-characterization, observations of drift collapse and overbreak, and a pre-1993 Q-system temporary support assessment (after Barton [1988]). Note the early use of Q-parameter histogram logging, a simple method of field logging used in the last 20 years.

These important aspects that are fundamental in caving initiation, can be studied by suitable combinations of block modeling (UDEC–BB) and block fracture modeling (FRACOD). There are also intimate cross-disciplinary links between this modelable "blockiness" and the resulting permeability, or "connectedness," and the resultant effects on seismic attenuation and its inverse Q_{seis} [Barton 2006].

EXTRAPOLATING Q USING SEISMIC REFRACTION PROFILES

Since there is a limit to how many boreholes can be drilled, how many cores can be logged, and how many permeability tests can be performed, it is useful to have alternative ways of estimating and extrapolating these point sources of information. This opinion applies, of course, to tunnels and to mining declines that can be reached, or almost reached, by boreholes or by deeply penetrating seismic refraction, with less constraints on energy sources than will be the case with civil engineering tunnels near population centers.

One may start by looking at correlation between velocity and measures of quality. Sjøgren et al. [1979] used seismic profiles (totaling 113 km) and local core logging results (totaling 2.9 km of core) to derive these helpful mean trends for hard rocks (Figures 8–11).

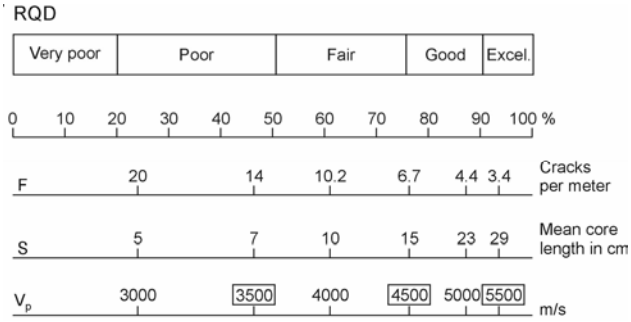

Figure 8.—Hard-rock, shallow seismic refraction. Sjøgren et al. [1979] combined 113 km of seismic profiles and 2.9 km of core logging to derive these mean trends for shallow tunnels.

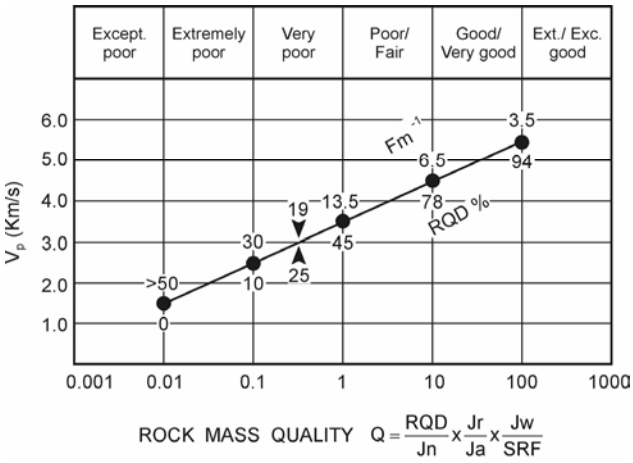

Figure 9.—Hard-rock, shallow seismic refraction, mean trends from Sjøgren et al. [1979]. The Q-scale was added by Barton [1995] using the hard-rock correlation $V_p \approx 3.5 + \log Q$. By remembering Q = 1: $V_p \approx 3.5$ km/s, and V_p = 3 km/s: Q ≈ 0.3, the Q–V_p approximation to a wide range of near-surface qualities is at one's fingertips (e.g., for hard, massive rock: Q = 100: $V_p \approx 5.5$ km/s, and when V_p = 5 km/s: Q ≈ 30).

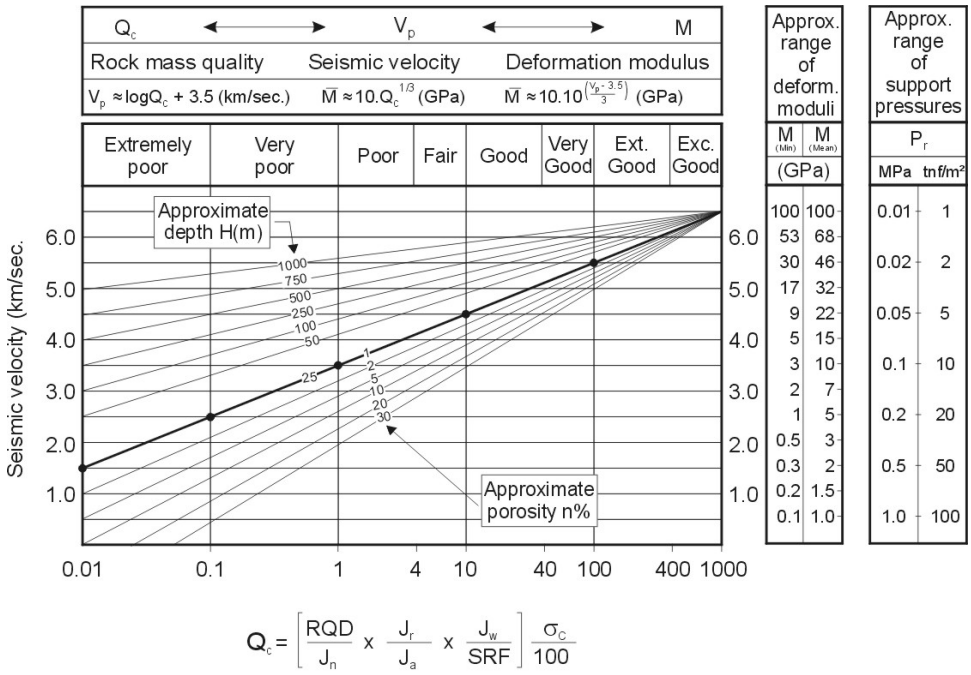

Figure 10.—An integrated empirical model for linking Q-value (via Q_c) to P-wave velocity, depth, matrix porosity, deformation modulus, and approximate support pressure (based on a mean $J_r = 2$). With this simplification, the independently derived Barton et al. [1974] support pressure formulation and the Barton [1995] deformation modulus formulation suggest inverse proportionality between support pressure and deformation modulus. This is logical, but the simplicity is nevertheless surprising [Barton 2002].

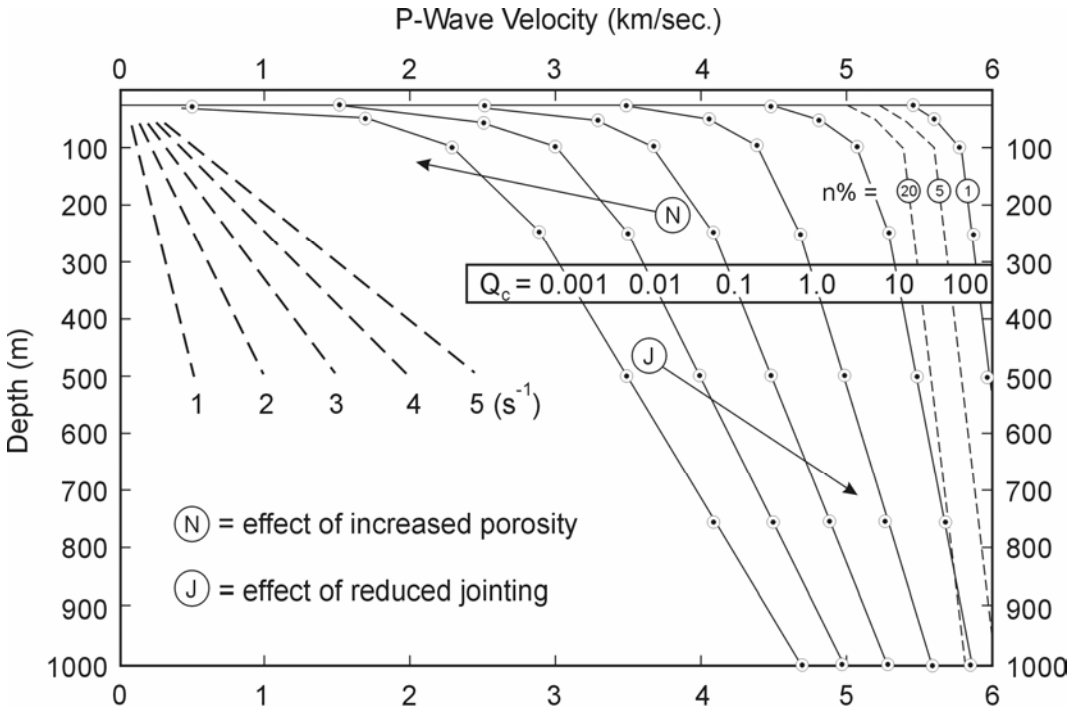

Figure 11.—The depth-velocity trends for different Q_c values. This graph explains why faulted rock ahead of a deep tunnel may sometimes be invisible or of such high velocity, like 4 km/s, that it is misinterpreted. It may subsequently cause tunnel collapse or trap a tunnel boring machine. In fact, such rock is still probably displaying an important contrast to the surrounding rock mass. In the case of soft rock, acoustic closure prevents such differentiation. In general, "Q-jumping" will be experienced when progressing downward to greater depth, i.e., rock qualities tend to improve, giving steeper V_p/depth (s^{-1}) gradients [Barton 2006].

TUNNEL AND DECLINE SUPPORT WHEN UNDER HIGH STRESS

The Q-system was developed from mostly civil engineering case records. Nevertheless, there are many tens of kilometers of semipermanent drifts and declines in most mines that have fundamentally similar needs to civil engineering tunnels, at least in their early years of life, before they become seriously affected by subsequent stress changes caused by the advancing mining front. In principle, one needs to design support (or select the correct support class) by classifying each round as the permanent mining drift or decline is driven. This is also a familiar task in civil engineering tunnels.

In mining situations, however, one may need to allow for future stress changes and deformations if a present location will soon become close to the mining front. The civil engineering approach of B+S(fr) for permanent roadways may need to be supplemented with longer fibers and probably the addition of mesh and cable bolts.

One must be prepared to reclassify and resupport if or when stress changes cause the need for rehabilitation due to observed deformation and cracking. The advancing mining fronts will tend to change the stress reduction factor (SRF), possibly to a dramatic level, causing apparent reductions to RQD and apparent or even real increases to J_n due to stress-fracturing effects. The addition of mesh and longer cable bolts for tolerating larger deformations will usually be a part of this subsequent phase. Longer fibers from the start that tolerate larger strains would be a logical difference of approach between civil and mining applications of B+S(fr) that might delay rehabilitation requirements.

Increases of SRF due to increased ratios of σ_1/σ_c with the advancing mining front *might* follow the changes suggested by Grimstad and Barton [1993] for the case of mining drifts in massive rock surrounding an ore body. The 1993–1994 (slightly) updated SRF ratings for high stress are shown in Table 1. If, on the other hand, the high stresses caused by mining depths or advancing mining fronts are acting on distinctly jointed rock, as experienced for instance in Western Australia, then the equations proposed by Peck [2000] are recommended. These are based on the original SRF values of 1974.

The exponential relationship derived by Peck [2000] from the original SRF ratings of Barton et al. [1974] is as follows:

$$\text{SRF} = 34(\sigma_c/\sigma_1)^{-1.2} \quad (1)$$

For strongly anisotropic stress fields, if measured, Peck [2000] derived the following best-fit equation from the Barton et al. [1974] suggestion of downgrading of σ_c with strong stress anisotropy:

$$\text{SRF} = 31(\sigma_1/\sigma_3)^{0.3}(\sigma_c/\sigma_1)^{-1.2} \quad (2)$$

Table 1.—Excerpt from updated SRF ratings based on Grimstad and Barton [1993], with additional notes from Barton [2002].

Case	Competent rock, rock stress problems	σ_c/σ_1	σ_θ/σ_c	Stress reduction factor (SRF)
H	Low-stress, near-surface, open joints.	>200	<0.01	2.5
J	Medium stress, favorable stress condition.	200–10	0.01–0.3	1
K	High-stress, very tight structure. Usually favorable to stability, may be unfavorable for wall stability.	10–5	0.3–0.4	0.5–2
L	Moderate slabbing after >1 hr in massive rock.	5–3	0.5–0.65	5–50
M	Slabbing and rock burst after a few minutes in massive rock.	3–2	0.65–1	50–200
N	Heavy rock burst (strain burst) and immediate dynamic deformations in massive rock.	<2	>1	200–400

NOTES:

1. For strongly anisotropic virgin stress field (if measured): When $5 \le \sigma_1/\sigma_3 \le 10$, reduce σ_c to 0.75 σ_c. When $\sigma_1/\sigma_3 > 10$, reduce σ_c to 0.5 σ_c, where σ_c = unconfined compression strength, σ_1 and σ_3 are the major and minor principal stresses, and σ_θ = maximum tangential stress (estimated from elastic theory).
2. Few case records available where depth of crown below surface is less than span width. Suggest an SRF increase from 2.5 to 5 for such cases (see case H).
3. Cases L, M, and N are usually most relevant for support design of deep tunnel excavations in hard massive rock masses, with RQD/J_n ratios from about 50 to 200.
4. For general characterization of rock masses distant from excavation influences, the use of SRF = 5, 2.5, 1.0, and 0.5 is recommended as depth increases from, say, 0–5 m, 5–25 m, 25–250 m, to >250 m. This will help to adjust Q for some of the effective stress effects, in combination with appropriate characterization values of J_w. Correlations with depth-dependent static deformation modulus and seismic velocity will then follow the practice used when these were developed.

STANDUP TIME USING Q–RMR CONVERSION

There is such widespread use of RMR, often in parallel with Q, that it is appropriate to address a possible interrelationship between the two. This, of course, has been the subject of many publications. One camp uses the "ln" (natural logarithm) format shown in Equation 1 in Figure 12; the other uses the "log" format shown in Equation 2 in this figure. Since the latter format is simpler and probably gives a more logical range of RMR in relation to the Q-scale (avoiding the negative values that occur below Q = 0.01), it has been used by the author also in relation to standup time and in relation to deformation modulus conversion between the two systems. Since we are engineers and not scientists, our craft is the ability to make realistic approximations, leaving unnecessary decimal places on the calculator.

The conversion between RMR and Q used to estimate standup time is based on Figure 12 (Equation 2). Figure 13 suggests that when the Q-value is as low as, for example, 0.01, or RMR is as low as 20, the standup time for a <1-m advance (beyond the last support) may be a matter of minutes, with collapse imminent or immediate if an advance of 2–3 m was made by an excessive length of blasting round.

SOME CHARACTERIZATION LESSONS FROM SITE INVESTIGATIONS

Lessons learned and Q-logging techniques applied when investigating ground conditions and modeling planned excavation and support of a mine-size cavern will now be reviewed. The case record is the 62-m span Gjøvik Olympic cavern in Norway. Reference will also be made to some of the Q-correlations given earlier in this paper.

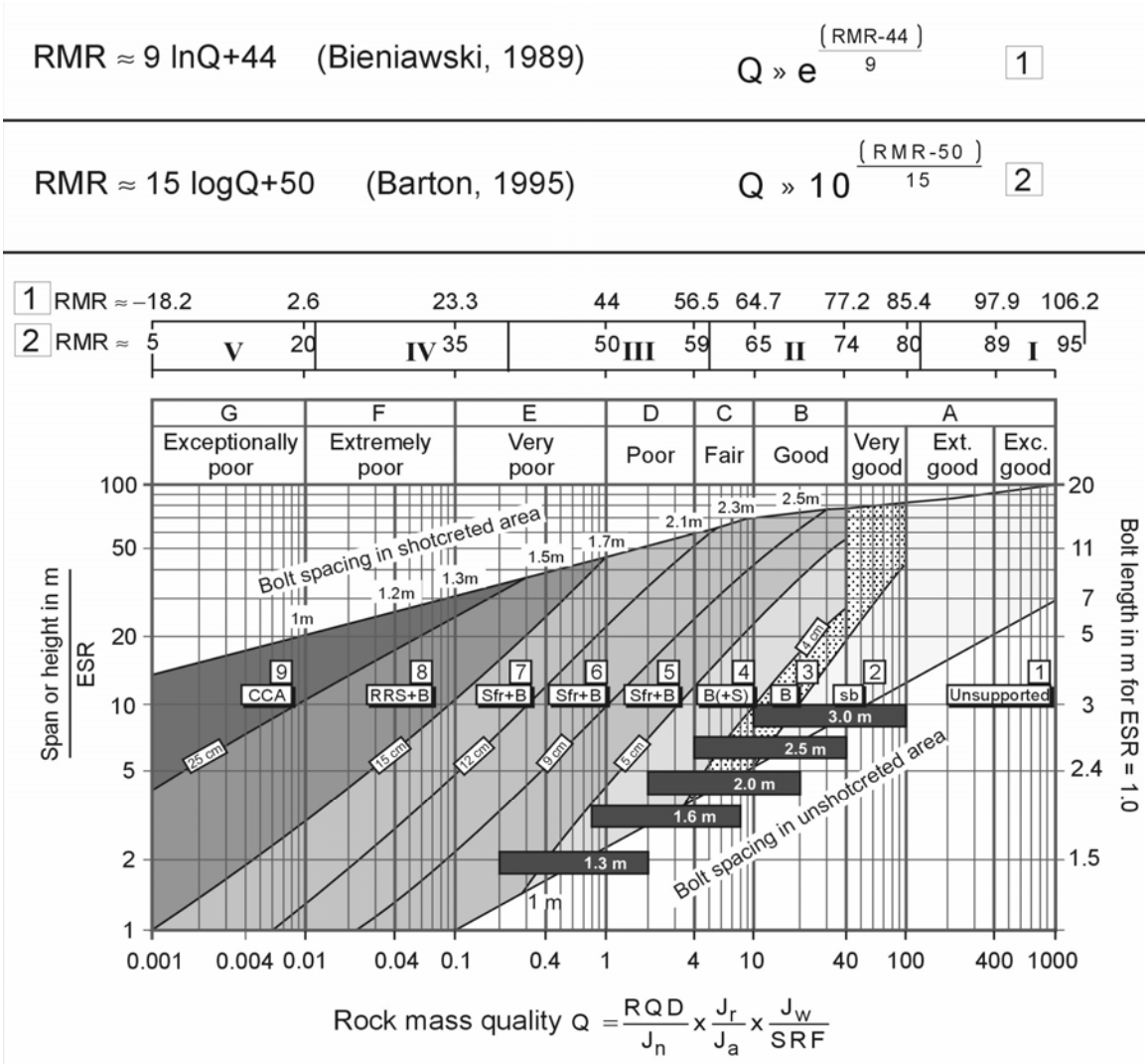

Figure 12.—The Q-support chart from the Grimstad and Barton [1993] update for S(fr) in place of S(mr). (NOTE: Equation 2 (inset) avoids unwanted negative values of RMR when Q < 0.01.) ESR = excavation support ratio.

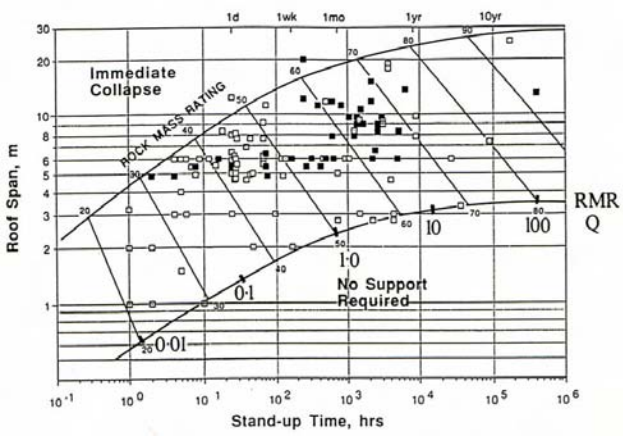

Figure 13.—Bieniawski [1989] standup time estimations. Note the Q-value approximations (large numbers next to small RMR numbers). "Roof span" refers to distance from the last support to the (new) tunnel face.

A start will be made with the comparison of Q-histogram-based core logging (see cross-hatched area in Figure 14) and the Q-logging performed in existing nearby excavations (see black area in Figure 14). Note the "tail" on the RQD distribution, as logged in the case of the core logging, and the lack of a tail when Q-logging in existing excavations. This was caused by lack of Q-parameter data where shotcrete covered the poorest rock when logging the existing excavations.

The boreholes used for core recovery were permeability tested (K mostly ≈ 10^{-7} to 10^{-8} m/s) and were also used for crosshole seismic tomography. Two examples are shown in Figure 15. The expected increase in velocity with depth, from about 3.5 to 5.0 km/s, is shown. What was

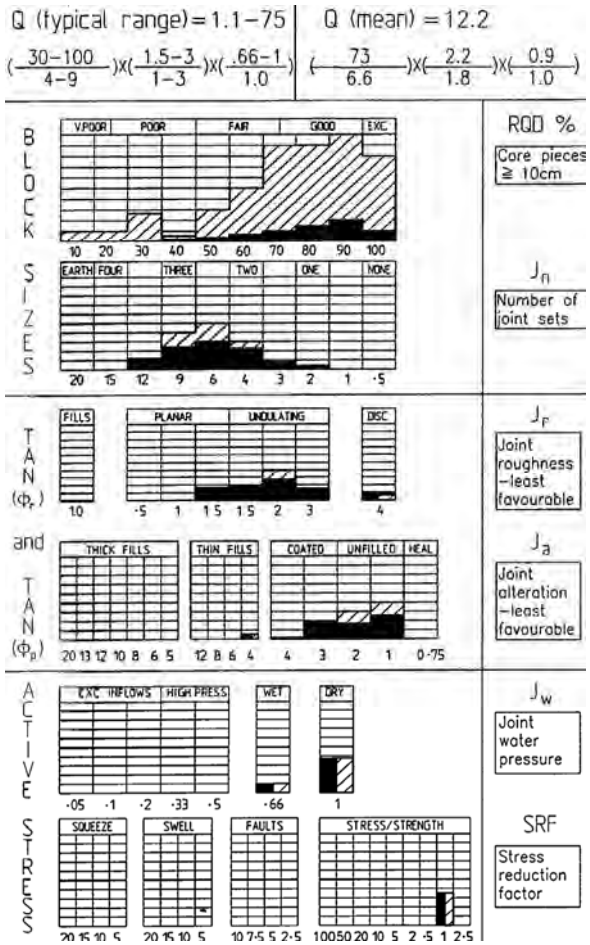

Figure 14.—Q-histogram logging of core (four holes) and existing local excavations (black), performed by different Norwegian Geotechnical Institute Q-loggers at different times [Barton et al. 1994].

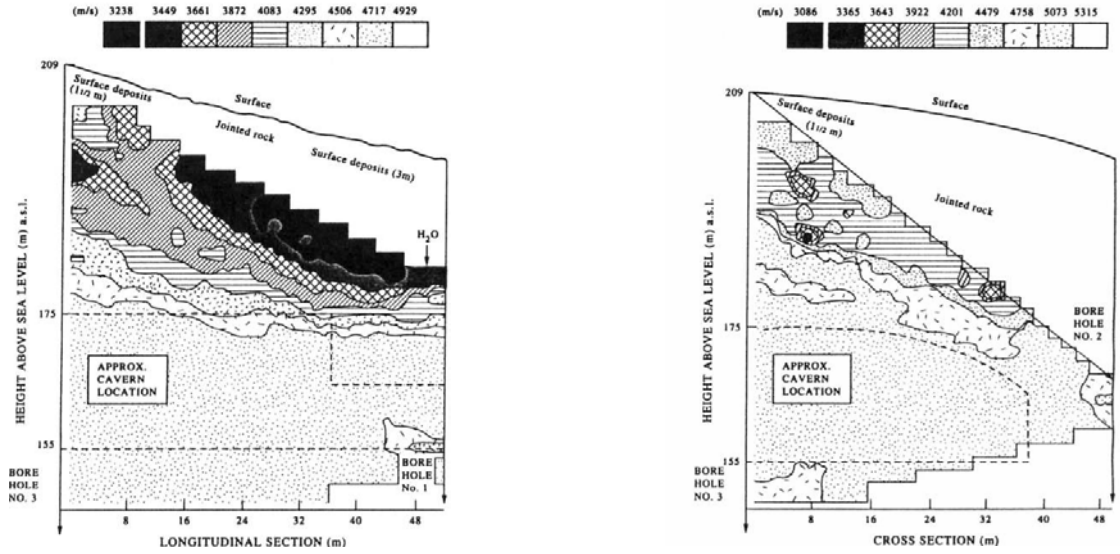

Figure 15.—Crosshole seismic tomography between two pairs of holes at the Gjøvik cavern site prior to cavern location decisions. An expected increase in velocity with depth is indicated, but in this particular case, the rock quality of the gneiss did not noticeably improve.

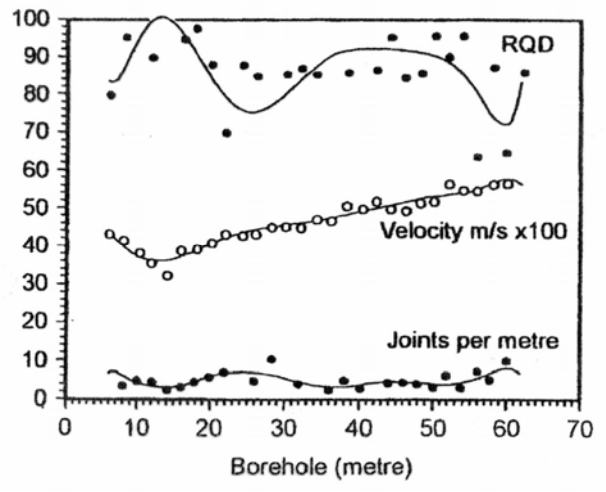

Figure 16.—Note the lack of a general rock quality improvement with depth compared to the consistent rise in P-wave velocity. The Q-value logged down the holes mostly varied between 1 and 30, with a mean of 10–12 and showed no tendency for improved quality below about 5 m [Barton et al. 1994].

unexpected was that the rock quality (RQD, Fm^{-1}, and Q) did not show a corresponding general increase in quality, as can be ascertained by studying Figure 16, which shows the velocities interpreted close to one of the boreholes.

The Q–V_p depth models shown earlier in Figures 10–12 indicated how velocity increase can occur without the need for Q-value increase. However, between 25 and 50 m, the predicted increase in velocity is relatively minor, such as 4.5–5.0 km/s. The increase of closer to 2 km/s between 10 and 60 m depth, shown in Figure 16, may be explained by the measured horizontal stress increase, which was as much as 5 MPa over this same limited depth range.

This increase, with little assumed change in rock quality, is possible due to the increased interlock of the rough conjugate jointing (high J_r and joint roughness coefficient (JRC)) and the relatively sound tectonized gneiss, with UCS about 90 MPa and joint compressive strength (JCS) about 75 MPa. In softer rock like chalk, acoustic closure (in relation to V_p) would occur at much shallower depths than this [Barton 2006].

INPUT DATA FROM ROCK MASS CLASSIFICATION

In the late 1960s, there was a movement in some rock mechanics circles to try to move beyond the confines of continuum modeling and focus on the possible effects of jointing on the performance and reinforcement needs of rock excavations, whether they be tunnels, slopes, or dam abutments. Thanks to the late-1960s modeling developments of R. E. Goodman and his colleagues with joint elements in finite-element codes, followed by P. A. Cundall in the early 1970s, first with μDEC, then UDEC, and later with 3DEC, this focus could be fulfilled by an increasing number of rock mechanics practitioners around the world. However, using these codes correctly, with realistic input data, needs experience, time, and therefore budgets to match. Ironically, input data for some continuum codes now seem to be considerably more complex than for discontinuum codes, as suggested in Figure 17.

$E_m\ (GPa) = \left(1 - \frac{D}{2}\right)\sqrt{\frac{\sigma_{ci}}{100}} \times 10^{((GSI-10)/40)}$	$E_m \approx 10 \times Q_c^{1/3}$
$\sigma'_{cm} = \sigma_{3l} \times \frac{(m_b + 4s - a(m_b - 8s))(m_b/4 + s)^{a-1}}{2(1+a)(2+a)}$	$\sigma_{cm} \approx 5\gamma Q_c^{1/3}$
$\phi' = \sin\left[\frac{6am_b(s + m_b\sigma'_{3n})^{a-1}}{2(1+a)(2+a) + 6am_b(s + m_b\sigma'_{3n})^{a-1}}\right]$	$\phi' \approx \tan^{-1}\left(\frac{J_r}{J_a} \times \frac{J_w}{1}\right)$
$c' = \frac{\sigma_{ci}[(1+2a)s + (1-a)m_b\sigma'_{3n}](s + m_b\sigma'_{3n})^{a-1}}{(1+a)(2+a)\sqrt{1 + \left(6am_b(s + m_b\sigma'_{3n})^{a-1}\right)/((1+a)(2+a))}}$	$c' \approx \left(\frac{RQD}{J_n} \times \frac{1}{SRF} \times \frac{\sigma_c}{100}\right)$

Figure 17.—The extraordinarily complex formulas *(left)* for developing input data for some recent continuum models compared with some of the less developed and equivalent Q-based formulas.

GSI-based Hoek-Brown formulations for "simple" geotechnical input data for the rock mass, shown in Figure 17, such as deformation modulus, cohesion, and friction angle, have reached "black box" levels of complexity, which seems to be detrimental to the idea of rock engineering if engineering judgment is still to be exercised in this rewarding field of engineering.

There is no possibility to have any feel for the influence of local rock quality on the rock mass compression strength, friction angle, or cohesion when formulations require software rather than estimation for their evaluation. The formulas on the left of Figure 17 cannot be considered "empirical" anymore, with the exception of the first equation for estimating modulus.

Presumably as a result of time and budgetary pressures, as well as the developing need to model large-scale mining problems, there has been a marked trend for using "convenient" continuum codes, which also have particularly good graphic representation of results. Simple software packages for handling the complex input data calculations (Figure 17) are also provided so that a smart user might theoretically need only limited understanding of rock mechanics principles to use the codes successfully.

The author has often used the method of rapidly left-thumbing from the back of a consultant's report to the front, whereby the colored appendices of endless stress distributions and deformation patterns can be read almost as in a film. Does all this color represent anything real?

Table 2.—Five hypothetical rock masses with reducing quality from top to bottom of the table.
(Note the difference between Q and Q_c due to normalization by $\sigma_c/100$. The sensitive, logical values of FC and CC already exist in the Q_c calculation, requiring no further empiricism.)

RQD	J_n	J_r	J_a	J_w	SRF	Q	σ_c	Q_c	FC, °	CC, MPa	V_p, km/s	E_{mess}, GPa
100.....	2	2	1	1	1	100	100	100	63	50	5.5	46
90.....	9	1	1	1	1	10	100	10	45	10	4.5	22
60.....	12	1.5	2	0.66	1	2.5	50	1.2	26	2.5	3.6	10.7
30.....	15	1	4	0.66	2.5	0.13	33	0.04	9	0.26	2.1	3.5
10.....	20	1	6	0.5	5	0.008	10	0.0008	5	0.01	0.4	0.9

Would the numerical modelers know how to input a neglected clay seam without "smoothing it out" in a continuum approximation? Would the complex estimates of c′ and φ′ in Figure 17 change very much?

CC AND FC: THE COHESIVE AND FRICTIONAL COMPONENTS OF Q_C

On the right side of Figure 17, simple Q-based equations for c and φ are shown that are actually found to be composed of each half of the Q_c-formulation. They have the advantage of not requiring software for their calculation—they already exist in the calculation of the Q_c value. They are defined as follows:

$$\text{cohesive component (CC)} = \text{RQD}/J_n \times 1/\text{SRF} \times \sigma_c/100$$
$$\text{frictional component (FC)} = \tan^{-1}[J_r/J_a \times J_w]$$

Examples of these rock mass component strengths are given in Table 2 for a range of possible Q-values for increasingly jointed rock masses.

The P-wave velocity and (pseudostatic) deformation modulus estimates in Table 2 are from the central diagonal, near-surface (25-m depth) interrelationships given in Figure 10. They could equally well be quoted for greater depths, if more relevant. Some physical examples of rock masses with different CC and FC characteristics are shown in Figure 18.

Plate loading tests taken to such high stress levels that rock mass failure occurs are rare. However, measurement of P-wave velocity at such sites may allow tentative extrapolation to other sites through a common rock mass quality estimate. Such data can then be a source of tentative rock mass strength ($\sigma_{c\,mass}$) estimation.

Table 3 suggests compressive (and cohesive) strengths in rock masses somewhat higher than those usually assumed. They also show some implicit variation from the values set up in Table 2 (from specific Q-parameter combinations), but reinforce the idea of potentially very high cohesive strengths (e.g., tens of MPa) in competent rock masses. This table of values seems to imply very different values of cohesion from some of the earlier RMR-based estimates of cohesion for rock masses, where c was generally given as <1 MPa for a wide range of RMR.

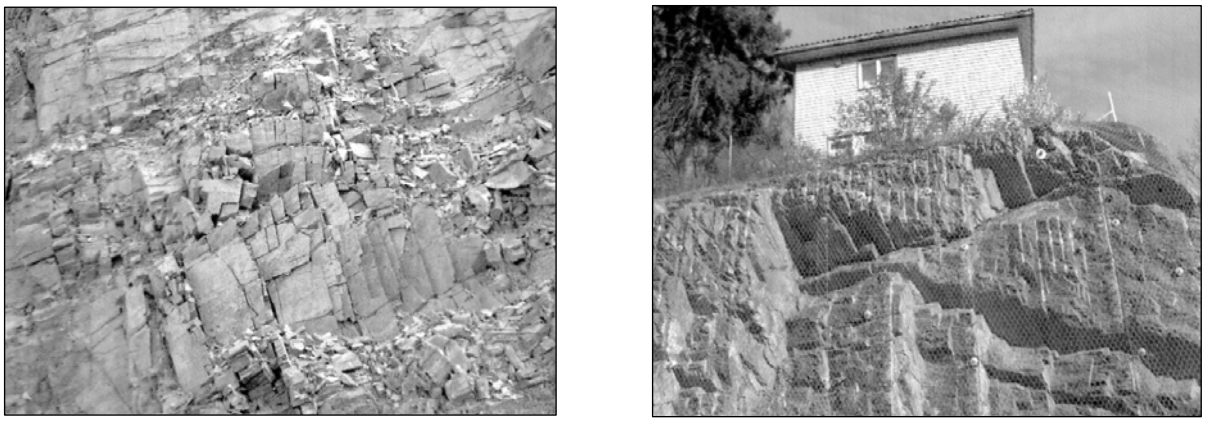

Figure 18.—Examples of rock masses with particularly low CC *(left)* and particularly low FC *(right)*. These require relatively more shotcrete *(left)* and relatively more bolting *(right)*. The original Q-system case records have apparently reflected these different needs, and the Q-parameter ratings developed have given the possibility of realistic CC and FC values.

Table 3.—Plate load tests driven to failure, with corresponding velocity and modulus data for the different rock masses
(Savich et al. [1974]; see Barton [2006] for other data sets)

Velocity V_p (km/s)	2.3	3.7	4.0
Modulus E_{mass} (GPa)	1	3	15
Rock mass σ_{cm} (MPa)	4	20	50

CONCLUSIONS

1. Q-system linkages to parameters useful for design are based on sound, simple empiricism that works because it reflects practice and that can be used because it can be remembered. It does not require black-box software evaluation.
2. The wide range of Q-values (0.001–1000) reflects to some degree the very wide range of geological conditions and is probably responsible for the fact that empirical equations based on the Q-value or on Q_c are particularly simple.
3. The Q-parameters J_n and J_r are very useful for evaluating overbreak potential and cavability in mining. When $J_n/J_r \geq 6$, significant overbreak will tend to occur, unless limited by timely support close to the excavation face. Caving is also likely to occur relatively unassisted. A modifying factor is, of course, the ratio J_r/J_a, representing frictional strength. Stress and water pressure are final modifiers.
4. An integration of the Q-value with seismic and permeability data has been developed because there is a limit to how many boreholes can be drilled, how many cores can be logged, and how many permeability tests can be performed. The ability to extrapolate these point sources of information helps to project rock quality classes along a tunnel or to different parts of a large cavern or mine.
5. Due to the effect of increased stress at greater tunnel or cavern depth, it must be expected that deformation modulus and seismic velocity will increase. Eventual sonic logging or crosshole tomography ahead of a tunnel face may therefore give a higher velocity than the rock quality may suggest.
6. Strength criteria of the form "c + tan φ" used in continuum codes, with links to GSI, have recently acquired remarkable complexity and require software for evaluation of their components. The terms CC and FC from the Q-calculation show promise in giving a direct preliminary estimate of the magnitudes of rock mass cohesive and frictional strength. Logic would suggest that these components should also not be *added* in an eventual failure criterion.

REFERENCES

Barton N [1995]. The influence of joint properties in modelling jointed rock masses. Keynote lecture at the Eighth International Society for Rock Mechanics Congress (Tokyo, Japan), *3*:1023–1032. Rotterdam, Netherlands: Balkema.

Barton N [1988]. Project Oscar – LKAB/LuH: Estimation of shear strength parameters for mine design studies. Oslo, Norway: Norwegian Geotechnical Institute, NGI report 87659–1.

Barton N [2002]. Some new Q-value correlations to assist in site characterization and tunnel design. Int J Rock Mech Min Sci *39*(2):185–216.

Barton N [2004]. Failure around tunnels and boreholes and other problems in rock mechanics [letter]. ISRM News J *8*(2):12–18.

Barton N [2006]. Rock quality, seismic velocity, attenuation and anisotropy. London and Netherlands: Taylor & Francis.

Barton N, By TL, Chryssanthakis P, Tunbridge L, Kristiansen J, Løset F, et al. [1994]. Predicted and measured performance of the 62-m span Norwegian Olympic ice hockey cavern at Gjøvik. Int J Rock Mech Min Sci Geomech Abstr *31*(6):617–641.

Barton N, Lien R, Lunde J [1974]. Engineering classification of rock masses for the design of tunnel support. Rock Mech *6*(4):189–236.

Bieniawski ZT [1989]. Engineering rock mass classifications: a complete manual for engineers and geologists in mining, civil and petroleum engineering. John Wiley & Sons, Inc.

Grimstad E, Barton N [1993]. Updating of the Q-system for NMT. In: Proceedings of the International Symposium on Sprayed Concrete – Modern Use of Wet Mix Sprayed Concrete for Underground Support. Oslo, Norway: Norwegian Concrete Association.

Hutchinson DJ, Diederichs MS [1996]. Cable bolting in underground mines. Bitech Publishers, Ltd.: Richmond, British Columbia, Canada.

Peck W [2000]. Determining the stress reduction factor in highly stressed jointed rock. Aust Geomech *35*(2).

Savich AI, Koptev VI, Zamakhaiev AM [1974]. In situ ultrasonic investigation of failure of limestone. In: Proceedings of the Third International Society for Rock Mechanics Congress (Denver, CO), IIA:418–423.

Sjøgren B, Øfsthus A, Sandberg J [1979]. Seismic classification of rock mass qualities. Geophys Prospect *27:* 409–442.